Applied Geochemistry 65 (2016) 22–35

Contents lists available at ScienceDirect

Applied Geochemistry

journal homepage: www.elsevier.com/locate/apgeochem

Geochemistry of organic-rich river waters in Amazonia: Insights on weathering processes of intertropical cratonic terrain

Adriana Maria Coimbra Horbe [a, b, *], Anderson da Silva Lages [b], Jean-Sébastien Moquet [c, d], Roberto Ventura Santos [a], Patrick Seyler [d], Gerard Cochonneau [e]

[a] Instituto de Geociências, Universidade de Brasília, Campus Universitário Darcy Ribeiro, Brasília, 70910-900, Brazil
[b] Programa de pós-graduação em Geociências, Universidade Federal do Amazonas, Av. Gal. Rodrigo O. J. Ramos 3000, Manaus, 69077-000, Brazil
[c] Instituto de Geociências, Universidade de São Paulo, Rua do Lago, 562 – Cidade Universitária, São Paulo, 05508-080, Brazil
[d] GET-OMP, IRD-CNRS-Université Toulouse 3, 14 avenue Edouard Belin, 31400 Toulouse, France
[e] ORE-HYBAM – GET (Géosciences Environnement Toulouse), UR234 IRD-Observatoire Midi-Pyrénées (OMP), France

ARTICLE INFO

Article history:
Received 27 January 2015
Received in revised form
20 October 2015
Accepted 22 October 2015
Available online 28 October 2015

Keywords:
Trace elements
Sr isotopes
O and D isotopes
Weathering rates
CO_2 consumption rate

ABSTRACT

In this study, eight organic-rich rivers that flow through the Brazilian craton in the southwestern Amazon rainforest are investigated. This investigation is the first of its type in this area and focuses on the effects of lithology, long-term weathering, thick soils, forest cover and hydrological period on the dissolved load compositions in rivers draining cratonic terrain. The major dissolved ion concentrations, alkalinity (TAlk), SiO_2, trace element concentrations, and Sr isotope contents in the water were determined between April 2009 and January 2010. In addition, the isotopic values of oxygen and hydrogen were determined between 2011 and 2013. Overall, the river water is highly dilute and dominated by the major dissolved elements TAlk, SiO_2 and K^+ and the major dissolved trace elements Al, Fe, Ba, Mn, P, Zn and Sr, which exhibit large temporal and spatial variability and are closely correlated with the silicatic bedrock and hydrology. Additionally, rainwater and recycled water vapor and the size of the basin contribute to the geochemistry of the waters. The total weathering flux estimated from our results is 2–4 t $km^{-2}.yr^{-1}$, which is one of the lowest fluxes in the world. The CO_2 consumption rate is approximately 21 –61 10^3 mol km^{-2} yr^{-1}, which is higher than expected given the stability of the felsic to basic igneous and metamorphic to siliciclastic basement rocks and the thick tropical soil cover. Thus, weathering of the cratonic terrain under intertropical humid conditions is still an important consumer of CO_2.

1. Introduction

Weathering of stable, cratonic terrain results in thick weathering profiles that isolate the parent rock from weathering, especially under intertropical humid conditions (e.g., Bardossy and Aleva, 1990; Tardy and Roquin, 1998 and references therein). The rivers that drain these regions are considered silicatic, with low weathering flux and low CO_2 consumption (Gaillardet et al., 1997; Millot et al., 2002; Oliva et al., 2003; Zakarova et al., 2007 and references within) relative to the rivers that flow through (Xu and Liu, 2010) or originate in (Edmond et al., 1996; Boeglin and Probst, 1998; Gaillardet et al., 1999; Moquet et al., 2014) tectonically unstable mountainous regions where intense mechanical erosion occurs and high concentrations of dissolved and suspended matter are observed. To understand the roles of cratonic terrain in the chemical cycle, it is important to quantify the dissolved load exported from cratonic terrain, understand how the terrain weathers, determine the CO_2 consumption rates of the terrain, and identify the main parameters that control the river water chemistry. Studying these topics is particularly important in Amazonia because this region supplies approximately 20% of the water (Callède et al., 2004), 10% of the dissolved load (Gaillardet et al., 2007) and 3% of the suspended load (Milliman and Syvitski, 1992) to the global ocean.

In Amazonia, the geochemistries of the Solimões-Amazon River and their larger tributaries have been well documented (e.g., Stallard and Edmond, 1983, 1987; Allègre et al., 1996; Edmond et al., 1996; Gaillardet et al., 1997; Mortatti et al., Probst, 2003; Moquet

* Corresponding author. Instituto de Geociências, Universidade de Brasília, Campus Universitário Darcy Ribeiro, Brasília, 70910-900, Brazil.
E-mail addresses: ahorbe@unb.br (A.M.C. Horbe), as.lages@hotmail.com (A.S. Lages), js.moquet@gmail.com (J.-S. Moquet), patrick.seyler@ird.fr (P. Seyler), gerard.cochonneau@ird.fr (G. Cochonneau).

http://dx.doi.org/10.1016/j.apgeochem.2015.10.007
0883-2927/

et al., 2011). However, information regarding mid-to small-scale cratonic tributary basins remains scarce. The most thorough geochemical studies were conducted by Hieronymus et al. (1993), Edmond et al. (1996) and Sondag et al. (2010). Although these studies did not characterize the relationship between water chemistry and bedrock composition, they highlighted the following main characteristics of the rivers draining the cratonic terrain in Amazonia: i) low suspended material concentrations; ii) elevated dissolved SiO_2, K^+, Al and Fe concentrations; iii) a pH of less than 7; and iv) weathering rates between 3.5 and 5 m Ma^{-1}. However, the diversity of the mineral paragenesis of the Brazilian craton, the length of time over which weathering occurred, the thick intertropical soils, the forest cover and the regional seasonality all influence the chemistry of the rivers. Thus, the main goal of our paper was to ascertain how these various factors regulate the chemical composition of river water, the weathering flux, migration of the weathering front and the CO_2 consumption rate. To explore this problem, we determined the water chemistry in two mid-to small-scale rivers hosted in cratonic environments in southwestern Amazonia, Brazil. Our results are helpful for understanding the spatial and temporal tropical weathering processes in the silicate cratonic terrain of Amazonia. Specifically, our results demonstrate how the geochemistry of medium-to-small drainage basins and the chemistry of the river water in these basins reflect the local environment and influence the main river.

2. Study area

The study area is located in the southwestern region of the Amazon basin between 6 and 13°S and 59–62°W (Fig. 1). The sampled rivers generally flow from south to north and belong to the Aripuanã basin in the west and the Sucunduri basin in the east (Fig. 1). The Aripuanã and Sucunduri Rivers in these two drainage basins drain into the Madeira River, which is one of the main tributaries of the Amazon River. These rivers drain lateritic terrain covered by rainforest, have very low suspended material concentrations and are classified as either organic rich or black waters according to the biochemical classification of rivers presented by Sioli (1968).

The Aripuanã drainage basin covers an area of 109,000 km^2 and extends for approximately 900 km in a north-south direction (Fig. 1). The mean discharge of the Aripuanã River, which empties the Aripuanã basin, is 2164 m^3 s^{-1} at the gauging station. At the gauging station, the Aripuanã River (Fig. 1, site 1) is nearly 400 m wide. The Aripuanã River mainly drains the western part of the study area. The Acari River, which is nearly 100 m wide at the sampling site (Fig. 1, site 6), the Jatuarana and Juma Rivers (sites 2 and 5, respectively), which are less than 30 m wide, and Ig1 and Ig2 (sites 3 and 4, respectively), which are less than 10 m wide at the sampling site, are all tributaries to the Aripuanã River.

The Sucunduri basin covers an area of 12 700 km^2 and is approximately 500 km long from south to north. The Sucunduri River has a mean discharge of 193 m^3 s^{-1} at the gauging station, where it is approximately 200 m wide (Fig. 1, site 8). The main tributary of the Sucunduri River is the Camaiú River (Fig. 1 site 7), which is 70 m wide at the sampling site.

The geology of the two basins is characterized by a variety of Proterozoic and Paleozoic silicate rocks (CPRM, 2013; Reis, 2006 and Fig. 1). In the study area, siliciclastic sedimentary rocks are located in the upper reaches of the Aripuanã drainage basin; felsic volcano-sedimentary rocks and intrusive felsic intrusive rocks (tonalite, granodiorite, and granite) with minor basic rocks (charnockite, amphibolite, and gneiss) are located in the middle of the basin; and siliciclastic sedimentary rocks are located near the sampling sites. The small tributaries (samples 2, 3, 4, and 5) and the Camaiú River (sample 7) flow entirely over siliciclastic sedimentary rocks, while the Acari River (sample 6) flows over felsic volcanic rocks (Fig. 1). The Sucunduri drainage basin is almost entirely composed of siliciclastic sedimentary rocks (siltstone, sandstone, claystone, siliceous breaches and minor dark grey limestone) and felsic volcano-sedimentary rocks (Fig. 1). All of these rocks have undergone long-term weathering, and have developed a residual lateritic crust composed of hematite, goethite, kaolinite, gibbsite and, occasionally, Mn minerals covered by oxisols and spodosols (Silva et al., 2012).

The climate is hot and humid and is slightly drier from May to September. The mean annual temperature ranges from 25 to 27 °C, the relative humidity is approximately 85%, and the yearly rainfall is 2336 mm $year^{-1}$ (data from the Brazilian Water National Agency's pluviometric station in the city of Humaitá, near the study area, from 1998 to 2007). Based on this 10-year record of rainfall, we have identified four main seasons: a wet season (during April, October, November, December and January with a mean rainfall of 265 mm $month^{-1}$), a receding water season (during May, with a mean rainfall of 156 mm^{-1}), a dry season (June, July and August, with a mean rainfall of 54 mm $month^{-1}$) and a rising water season (during September, with a mean rainfall of 163 mm $month^{-1}$). The wet and dry seasons correspond to higher and lower river discharge. Human pollution does not significantly affect the region due to the very low population density (<5 individuals km^{-2}). However, some anthropogenic impacts may occur in the town of Apuí and along the road and in deforested areas.

3. Materials and methods

River water samples were collected monthly from April 2009 to January 2010 along the Transamazonica highway near the town of Apuí in southwestern Amazonia, Brazil (Fig. 1). In addition, a spring was sampled to evaluate the geochemical characteristics of the local groundwater and to determine its influence on the river water (Fig. 1). Samples were collected from the middle of each river. The Aripuanã and Sucunduri Rivers were sampled from a canoe, and the other rivers were sampled from bridges. Each water sample was collected in a plastic bag, from which a subsample of water was collected using a 20 ml syringe. Next, the sample was passed through a 0.45-μm Millex filter before storing in a polyethylene flask. Each flask was prepared by soaking in a 10% HNO_3 solution for 24 h, rinsing three times with ultrapure water and then rinsing again three times with the sampled water. Two flasks were used for each sample. In the first flask, 0.02 g of thymol was added to prevent bacterial action. The sample in the first flask was analyzed for major ions, total alkalinity and SiO_2. In the second sample flask, which was used for trace element analysis, two drops of bi-distillated HNO_3 were added to prevent precipitation.

Electrical conductivity, pH, total alkalinity (TAlk; samples at pH > 4.3 were titrated with sulfuric acid), SiO_2 (by spectrophotometry), cations (Na^+, K^+, Mg^{2+}, and Ca^{2+}) and anions (Cl^-, NO_3^-, and SO_4^{2-}) were determined for all samples with a reproducibility of ±5%. Ions were analyzed using a DIONEX ICS 900 ion chromatograph calibrated with a DIONEX standard-compliant solution. Trace elements (Ag, Al, As, Au, Ba, B, Be, Bi, Cd, Co, Cr, Cu, Fe, Ga, Ge, Hf, Hg, In, Mn, Mo, Ni, Nb, P, Pb, Pt, Rb, Re, Rh, Ru, Sb, Sc, Se, Sn, Sr, Ta, Te, Tl, V, Zn, Zr, and Y) and rare earth elements (REEs) were determined for samples collected in December (high water), May (receding water), July (low water) and September (rising water) using inductively coupled plasma mass spectrometry (ICP-MS) at ACMELAB in Vancouver, Canada. TMDA-70 was used as a standard.

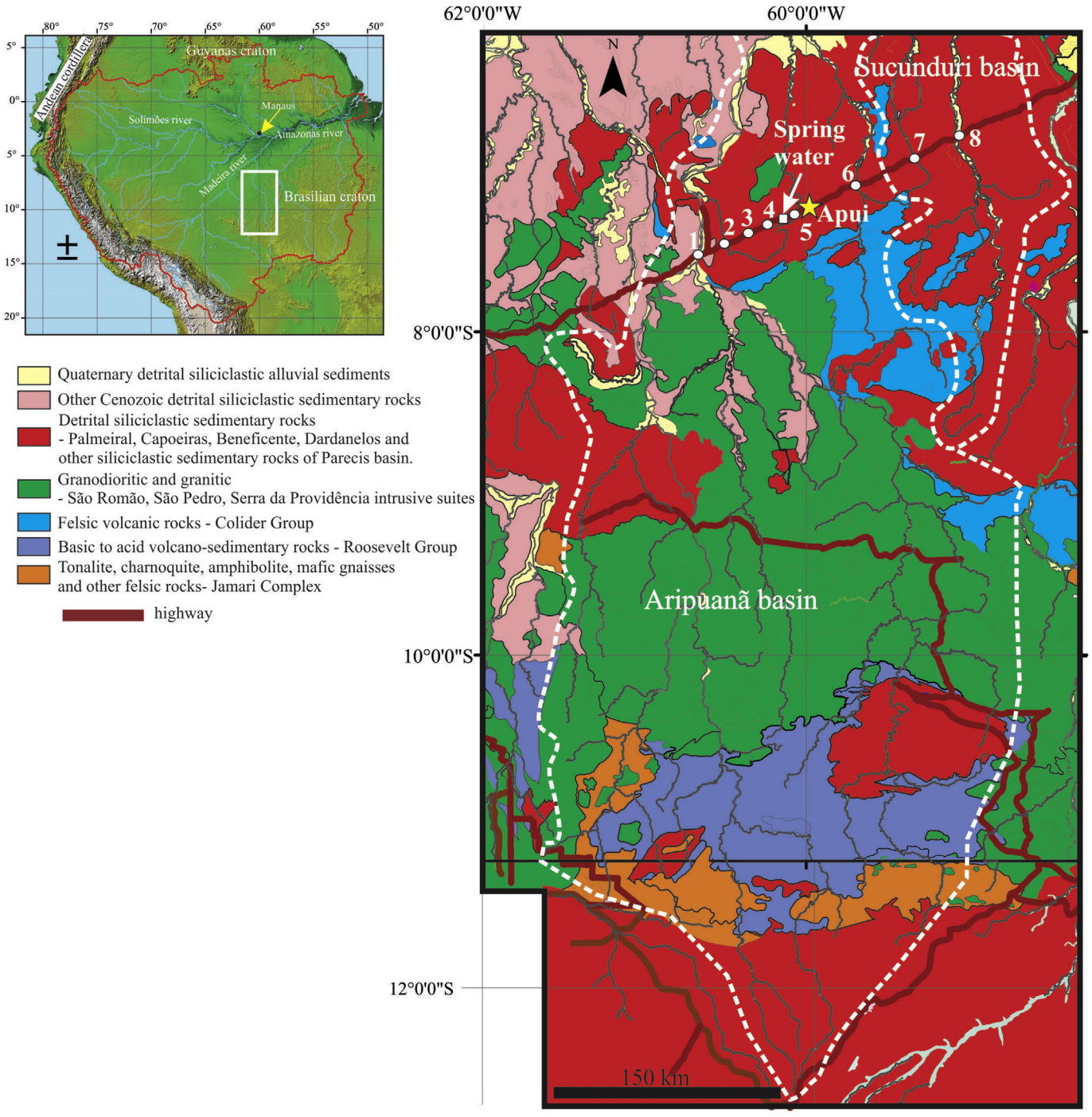

Fig. 1. Map of the locations of the Aripuanã and Sucunduri drainage basins showing a simplified geologic setting and the locations where the river samples were collected. The white points indicate the sampling locations: 1. Aripuanã, 2. Jatuarana, 3. Ig1, 4. Ig2, 5. Juma, 6. Acari, 7. Camaiú and 8. Sucunduri. The white square indicates the spring sample.

Strontium isotopes were separated and purified by chromatographic column separation (resin AG 50W-X8) before loading onto a tungsten filament with a TaF-solution and onto double rhenium filaments with silica gel and H_3PO_4 (0.1 M). The Sr isotope ratios were measured using a Thermal Ionization Mass Spectrometer (Finningan MAT-262 Thermo Scientific, Bremen, Germany) at the GET Laboratory in Toulouse, France, and the NBS 987 standard was measured alongside the samples. Oxygen and hydrogen isotopes were measured over nine months (in July, September and December of 2012, May, August and November of 2012 and March, April and June of 2013). The analyses were performed at the Universidade de Brasília in Brazil by using Thermo Finnigan Delta V and CRDS-Picarro mass spectrometers. The analytical procedure was described previously by Gupta et al. (2009).

Statistical analyses were conducted using Statistica 9.0 software and the single linkage Euclidian distance to determine the similarities among the samples. The averages of each major dissolved element and the trace elements were weighted by the amount of monthly rainwater.

The atmospheric contribution was corrected using the following

equation (Meybeck, 1983):

$$C = Cx_{river} - \left(\left(Cx/CCl^{-}\right)_{sea} \times CCl^{-}_{river}\right)$$

where Cx represents the elemental concentration and CCl^{-} represents the chloride concentration. The Cx/CCl^{-} value of the seawater was obtained from Berner and Berner (1987). This correction, which is one of three possible atmospheric corrections (Gaillardet et al., 1997, 1999; Moquet et al., 2011), was used because no salt-bearing rocks were present in the study area (CPRM, 2013, Reis, 2006) and because the Cl^{-} concentration was less than 760 μg L^{-1} (or 20 μmol L^{-1}).

Because the studied basins have silicate lithology, the remaining dissolved solids can be considered as resulting from silicate weathering. Thus, the chemical weathering rates calculated hereafter correspond to the silicate chemical weathering rates.

The chemical weathering rate (CWR) and CO_2 consumption rate were calculated using the following equations:

$$CWR = Qmean/S \times CWC \text{ and } CO_2\ rate = Qmean/S \times CO_2$$

where the CWR and CO_2 consumption rate are presented in t km^{-2} yr^{-1}, Q (mean annual discharge) and m^3 yr^{-1}, and S (drainage area) is presented in km^2. The CWC is the chemical weathering concentration and was determined from the total $Na^+ + K^+ + Ca^{2+} + Mg^{2+} + SiO_2$ in mg L^{-1}. The CO_2 term (theoretical concentration of CO_2 consumed from silicate weathering) was calculated from $Na^+ + K^+ + Ca^{2+} + Mg^{2+}$ in μmol L^{-1} after correcting for atmospheric inputs (Table 2).

The migration of the weathering front (Table 3) was calculated from $Na^+ + K^+ + Ca^{2+} + Mg^{2+} + SiO_2$ in mg L^{-1} after correcting for atmospheric contributions (Table 2) and the average silicate rock density (2.7 g cm^{-3}, Xu and Lui, 2010).

River discharge data were obtained from the ORE-HYBAM web site (www.ore-hybam.org) for the Aripuanã (gauging station Prainha Velha), Acarí (gauging station BR 230) and Sucunduri (gauging station Sucunduri) Rivers. For the other rivers without gauging stations, we estimated the discharge based on the relative size of the river. Thus, the discharge of the Jatuarana River was estimated to equal one quarter of the discharge of the Acarí River and the discharge of the Juma and Camaiu Rivers was estimated equal half the discharge of the Acarí River.

4. Results

4.1. Major dissolved elements

The river waters are acid to neutral (pH = 3.7 to 7.2) and have very low conductivities (8.2–28 μS cm^{-1}) (Table in Supplementary data files). The water in the Aripuanã and Acari Rivers is less acidic (4.7–7.2) than the water in the other rivers. Overall, the conductivity of the spring water is higher (14.3–64.6 μS cm^{-1}) than the conductivity of the river water. Following the normalized inorganic charge balance (NICB), which considers the charges of the major dissolved elements, the sampled waters are imbalanced and usually exhibit excess anions due to the undosage of organic acids (NICB = −0.4 to −11.7) (Supplementary data files).

On a cation ternary diagram, the samples are clustered at the $Na^+ + K^+$ apex, which accounts for nearly 65–95% of the total cation composition in most of the samples (Fig. 2A). In addition, the K^+ concentrations are up to eight times higher than the Na^+ concentrations (Table 1 and Supplementary data files). In the SiO_2+TAlk + anion ternary diagrams, most of the samples are clustered towards the TAlk apex (Fig. 2B), which accounts for up to 80% of the anion and SiO_2 content. For the samples where TAlk was not analyzed (pH < 4.3), SiO_2 accounted for at least 20% of the anion and SiO_2 content. This river chemistry is similar to the chemistry of the rivers flowing through cratonic terrain and forested regions, such as the Congo-Zaire, Niger, Tocantins and Negro Rivers (Gaillardet et al., 1999) and several tributaries of the Orinoco River (Edmond et al., 1996) (Fig. 2).

Fig. 3 shows large monthly chemical fluctuations between the rivers, especially when compared with the spring water. The H^+ content and pH are lower from June to November, which is the seasons of low and rising water. This result indicates a positive correlation (r = 0.7) with discharge (the discharge values were calculated by averaging the monthly discharges of the Aripuanã, Acari and Sucunduri Rivers from 2001 to 2009). The low pH (<4.3) and consequential absence of TAlk measurements in the samples from November to May, especially in the Ig1, Ig2, Juma and Sucunduri Rivers, indicate that a dilution effect also influences the total dissolved solids (TDS). The concentration of SiO_2 remains nearly constant for 10 months, which indicates that the leaching rates of SiO_2 do not depend on the hydrological cycle. Between June and November (the seasons of low and rising water), the concentrations of Ca^{2+}+Mg^{2+} are lower in the Ig1, Ig2 and Camaiú Rivers and in the spring waters. The Aripuanã and Acari Rivers have greater TDS concentrations and lower TDS variability, while the smaller rivers (Ig1, Ig2 and Juma) have the most variable TDS (Fig. 3). The spring water has the highest H^+ and NO_3^- concentrations, the lowest SiO_2 concentrations and the most variable Na^++K^+, Cl^-, and SO_4^{2-} concentrations.

4.2. Dissolved trace elements

Al and Fe are the most concentrated trace elements. Together, Ba, Mn, P, Zn, Sr, Al and Fe represent nearly 100% of the dissolved trace element load (Supplementary data files). Most of the river

Table 1
Geographical and hydrological characteristics of the studied rivers.

Sample number	River name	Latitude	Longitude	Large	Litology % (CPRM, 2013)	
		S	W	m	Siliciclastic sedimentary rocks	Volcano-sedimentary, felsic and minor basic and limestone rocks
1	Aripuanã	07°31′24″	60°40′13″	400	30	70
2	Jatuarana	07°27′48″	60°30′20″	30	100	–
3	Ig 1	07°20′34″	60°14′32″	10	100	–
4	Ig 2	07°16′45″	60°03′24″	10	100	–
5	Juma	07°12′43″	59°55′20″	30	100	–
6	Acari	07°06′10″	59°41′26″	100	5	95
7	Camaiú	06°56′00″	59°19′45″	70	95	5
8	Sucunduri	06°47′41″	59°02′34″	200	90	10
	Spring water	07°18′05″	60°04′57″	–	100	

Table 2
Average geochemical composition of the river water and groundwater weighted by the amount of the rainwater in μg L^{-1}, in μmol L^{-1}, after atmospheric contributions, % of the ions amount provided by the atmosphere, Mg/Na and Ca/Na ratios in μmol L^{-1}.

	Ions	Aripuanã	Jatuarana	Ig 1	Ig 2	Juma	Acari	Camaiú	Sucunduri	Average	Spring water
μg L^{-1}	H^+	9	28	115	110	43	11	33	53	51	139
	Na^+	1142	137	152	547	569	1147	248	268	527	872
	K^+	1485	1279	686	1267	1582	3066	2102	2220	1711	682
	Ca^{2+}	1043	1236	157	620	919	823	122	1136	757	422
	Mg^{2+}	487	437	141	117	398	382	173	661	350	102
	SiO_2	4395	3266	2416	2764	3161	5568	2717	3495	3473	1428
	TAlk	13429	5647	2637	2512	3062	9847	6204	5671	6126	1042
	Cl^-	325	293	248	1732	50	298	308	226	300	580
	NO_3^-	1019	630	469	41	999	796	1794	1584	1128	4786
	SO_4^{2-}	181	200	91	141	237	150	128	147	159	279
	TDS	23517	13155	7112	10137	11345	22090	13829	15460	14581	10331
	Cation + SiO_2	8553	6356	3552	5315	6629	10987	5362	7780	6817	–
	Cation + $SiO_2{}^*{}_H$	9287	4888	3694	4488	5921	9891	6164	6644	6372	–
	Cation + $SiO_2{}^*{}_L$	11618	8083	5153	5198	8622	13940	6616	8824	8507	–
μmol L^{-1}	H^+	8.80	27.55	114.73	110.03	42.58	11.96	33.31	52.72	50.21	139.09
	Na^+	49.68	5.98	6.63	23.81	24.74	49.91	10.79	11.67	22.90	37.94
	K^+	37.98	32.72	17.54	32.41	40.47	78.43	53.76	56.78	43.76	17.44
	Ca^{2+}	26.03	30.85	3.92	15.46	22.94	20.54	3.04	28.35	18.89	10.52
	Mg^{2+}	20.04	17.99	5.82	4.80	16.37	15.72	7.12	27.20	14.38	4.19
	SiO_2	73.15	54.35	40.20	46.00	52.61	92.68	45.22	58.17	57.80	23.77
	TAlk	220.09	92.55	43.21	41.17	50.19	161.37	101.68	92.93	100.40	17.07
	Cl^-	9.18	8.27	6.99	9.21	10.56	8.40	8.67	6.39	8.46	16.36
	NO_3^-	16.45	10.16	7.57	27.94	16.12	12.84	28.94	25.55	18.19	77.18
	SO_4^{2-}	2.92	4.33	2.09	2.98	3.59	3.01	2.07	2.78	2.97	4.51
	TDS	464.33	284.76	248.70	313.81	280.16	454.85	294.60	362.53	337.97	348.08
Ions amount after atmospheric contribution in μmol L^{-1}	Na^+	41.80	−1.12	0.62	15.90	15.67	42.70	3.34	6.19	18.50	23.90
	K^+	37.81	32.57	17.41	32.24	40.27	78.27	53.60	56.66	32.06	17.13
	Ca^{2+}	25.86	30.70	3.79	15.29	22.74	20.38	2.87	28.23	19.68	10.21
	Mg^{2+}	19.15	17.19	5.14	3.90	15.34	14.90	6.28	26.58	12.14	2.60
	SiO_2	73.15	54.35	40.20	46.00	52.60	92.67	45.21	58.17	53.26	23.77
	TAlk	220.05	92.52	43.18	41.13	50.15	161.34	101.65	92.91	0.00	17.01
	Cl^-	0.00	0.00	0.00	0.00	0.00	0.00	0.00	0.00	89.41	0.00
	NO_3^-	16.45	10.16	7.57	27.94	16.12	12.84	28.94	25.55	15.65	77.18
	SO_4^{2-}	2.44	3.90	1.73	2.50	3.05	2.57	1.62	2.45	2.7	3.66
	TDS	436.72	241.39	119.64	184.92	215.94	425.68	243.52	296.73	239.72	175.46
	Cations	124.62	80.45	26.96	67.34	94.03	156.26	66.10	117.65	82.38	–
	Cations$^*{}_H$	127.38	50.79	30.46	55.40	83.59	136.54	78.11	86.97	81.16	–
	Cations$^*{}_L$	140.72	94.68	41.24	33.24	86.32	126.96	73.35	114.66	88.90	–
μg L^{-1}	Cation + SiO_2	8336	6187	3387	5098	6380	10789	5157	7630	5878	–
	Cation + $SiO_2{}^*{}_H$	9066	4734	3530	4294	5701	9692	5920	6476	6177	–
	Cation + $SiO_2{}^*{}_L$	11397	7978	5043	5061	8486	13854	6520	8752	8386	–
Provided by the atmosphere in %	Na^+	16	100	91	33	37	14	69	47	59	
	K^+	0	0	1	1	0	0	0	0	1	
	Ca^{2+}	1	1	3	1	1	1	5	0	1	
	Mg^{2+}	4	4	12	19	6	5	12	2	9	
	SiO_2	0	0	0	0	0	0	0	0	0	
	HCO_3^-	0	0	0	0	0	0	0	0	0	
	Cl^-	100	100	100	100	100	100	100	100	100	
	NO_3^-	0	0	0	0	0	0	0	0	0	
	SO_4^{2-}	25	21	38	32	22	28	34	22	28	
	TDS	4	6	11	9	9	4	7	4	8	
	Ca/Na	0.62	–	6.10	0.96	1.45	0.48	0.86	4.56	2.3	0.43
	Mg/Na	0.46	–	8.26	0.25	0.98	0.35	1.88	4.29	2.5	0.11

TAlk-total alkalinity; H- for the high water season; L-for the low water season.

waters have lower concentrations in May (except the Aripuanã River) during the receding season (Supplementary data files), which indicates that dilution occurs with increasing discharge. In the Sucunduri River and in the spring water, higher concentrations were observed in July (during low water season). In contrast, higher concentrations were observed in September (during rising water season) in the smallest rivers (Ig1 and Ig2) and in December (during high water season) in the other rivers. During at least three seasons, the Ig1 and Juma Rivers have the highest Fe and Mn concentrations, the Jatuarana and Juma Rivers have the highest Al concentrations, the Ig1 River has the highest Zn concentration, and the Aripuanã, Acari and Sucunduri Rivers have the highest Ba concentrations. The highest REE concentrations occurred in September (during the rising water season) and December (during the high water season). The most concentrated elements are La and Ce (Supplementary data files). The La and Ce concentrations vary in phase with Mn, with higher concentrations in September (Supplementary data files).

To compare the water chemistry to the local bedrock composition, the trace elements were normalized to the estimated average composition of the upper continental crust (Taylor and McLennan, 1985). The results showed a positive Zn anomaly and a negative Zr anomaly, despite variations in their absolute concentrations (Fig. 4). The positive Zn anomaly was observed in all river waters, higher Mn concentrations were observed in the Ig1 and Juma Rivers, and higher Cu concentrations were observed in the Acari River, which indicate that these trace element concentrations were probably related to the occurrence of sulfide and manganese in the region

Table 3
Weathering chemical rates, denudation chemical rates and CO_2 consumption.

Mean	Drainage area km^2	Annual discharge* m^3 s^{-1}	Runoff mm yr^{-1}	Chemical weathering rate t km^{-2} yr^{-1}	Chemical denudation rate m Ma^{-1}	Total CO_2 rate 10^3 mol km^{-2} yr^{-1}
Aripuanã						
1 year	140648	2164	486	4.15	1.50	60.51
High water season	140648	4195	941	8.74	3.16	119.90
Low water season	140648	1134	254	2.96	1.07	35.81
Jatuarana						
1 year	2019	30	469	2.98	1.07	37.72
High water season	2019	55	856	4.18	1.50	43.46
Low water season	2019	10	152	1.23	0.45	14.43
Juma						
1 year	5652	60	335	2.22	0.79	31.50
High water season	5652	110	611	3.62	1.29	51.10
Low water season	5652	20	109	0.94	0.34	9.40
Acari						
1 year	13421	120	282	3.10	1.13	44.09
High water season	13421	219	515	5.09	1.24	70.31
Low water season	13421	39	92	1.28	0.47	11.64
Camaiú						
1 year	5810	60	326	1.75	0.62	21.54
High water season	5810	110	595	3.67	1.30	46.45
Low water season	5810	20	106	0.70	0.26	7.77
Sucunduri						
1 year	17059	193	357	2.78	1.01	42.01
High water season	17059	450	832	5.53	2.00	72.40
Low water season	17059	91	168	1.49	0.55	19.30
Annual mean				3.76	1.37	54.60

* water discharge for 10 year-term averages (2000–2009) are from www.ore-hybam.org, station Prainha Velha for Aripuanã river, station BR 230 for Acarí river and station Sucunduri for Sucunduri river. For the Jatuarana River was used one quarter of the discharge of the Acarí River and for Juma and Camaiu Rivers were used the half discharge of the Acarí river. Total craton area 2.5.10^6 km^2 total Amazon basin area 6.10^6 km^2.

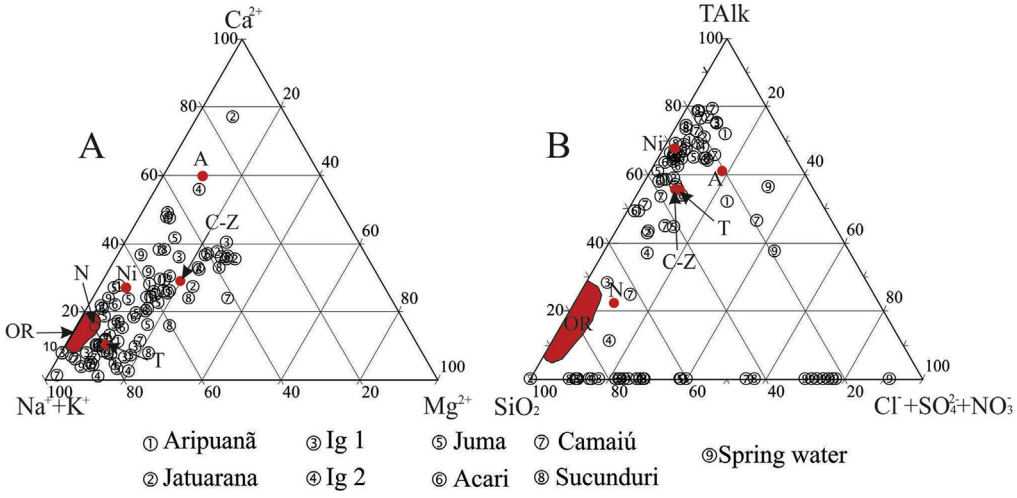

Fig. 2. Ternary diagrams showing the compositions of the cations (A) (μg L^{-1}) and anions + SiO2 (μg L^{-1}) (B). Comparison of the rivers flowing through the cratonic terrain (red points): the Congo and Zaire Rivers (C–Z), Tocantins River (T), Niger River (Ni), Negro River (N), and Amazonas River (A) (Gaillardet et al., 1999) and tributaries of the Orinoco River (OR) from Edmond et al. (1996). (For interpretation of the references to colour in this figure legend, the reader is referred to the web version of this article.)

(CPRM, 2013; Reis, 2006 and Silva et al., 2012). The probable sulfide source for Zn is indicated by the higher SO_4^{2-} during December, when the Zn concentration was also the highest (Supplementary data files). Thus, although further investigations are needed to

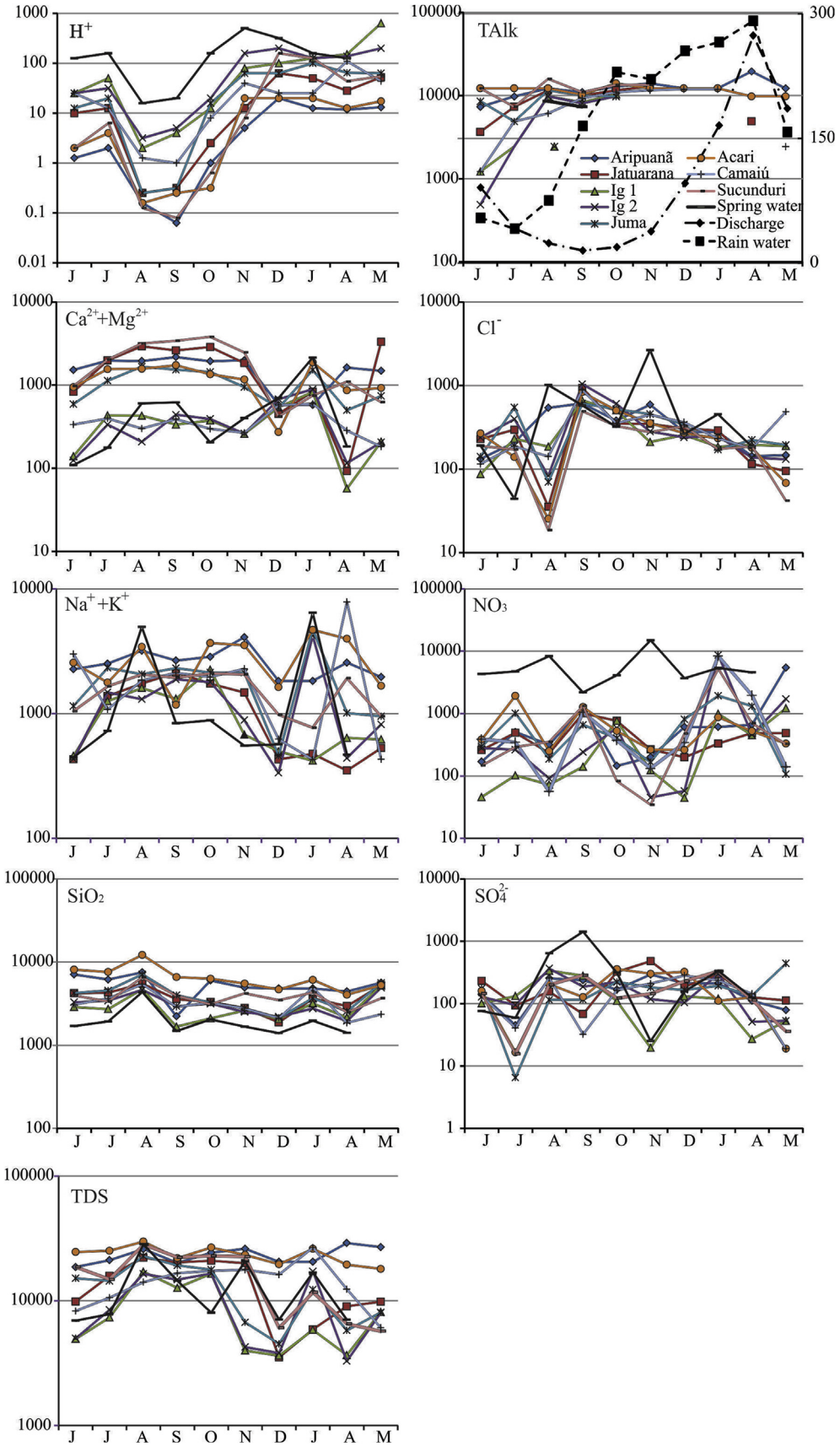

Fig. 3. Monthly major dissolved elements (μg L^{-1}). The discharge values were calculated using the average monthly discharge from the Aripuana, Acari and Sucunduri Rivers from 2001 to 2009.

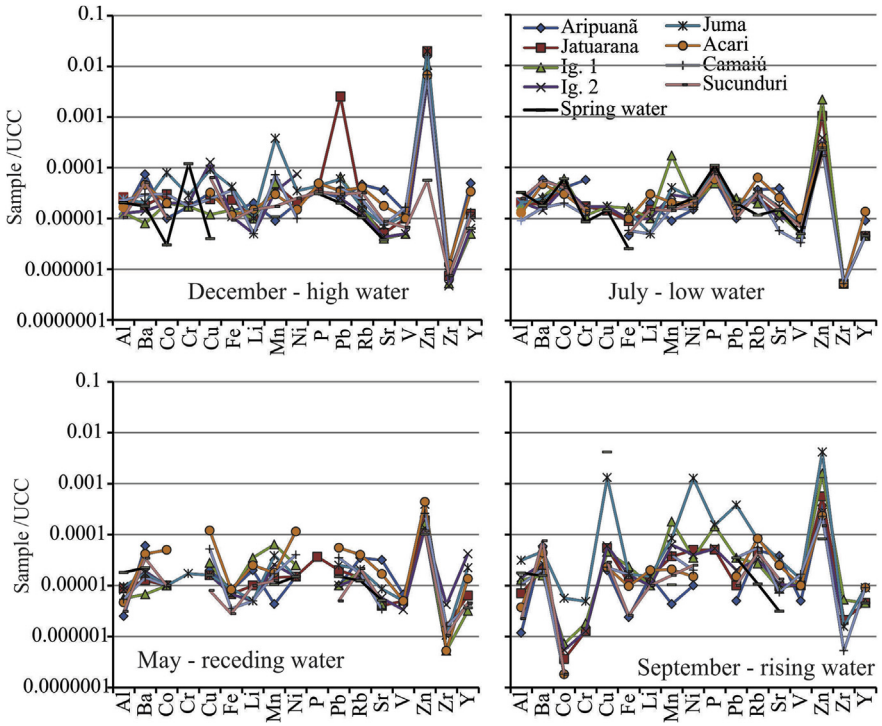

Fig. 4. Trace element concentrations normalized to the estimated average composition of the upper crust (UCC, Taylor and McLennan, 1985).

confirm this hypothesis, the abundances of these elements indicate the influence of the bedrock and suggest that river water chemistry can be used as an exploration tool for Mn and sulfide deposits in the region.

The REEs were also normalized to the estimated average composition of the upper continental crust (Taylor and McLennan, 1985). The results showed a flat pattern, except for a positive Ce anomaly in December in the Jatuarana River, positive La anomalies in May and September in most of the rivers and a positive Eu anomaly in the Juma River in May (Fig. 5). The REE fractionation patterns have some similarities with the fractionation pattern of the Negro River, which is also an organic river, and with the Solimões-Amazonas River and the rivers of Central Africa (Dupré et al., 1996; Gaillardet et al., 1997; Viers et al., 2000; Barroux et al., 2006).

4.3. Sr isotopes

The lowest $^{87}Sr/^{86}Sr$ ratio was observed in the Aripuanã River, and the highest ratio was observed in the Sucunduri River (Fig. 6). In addition, the $^{87}Sr/^{86}Sr$ ratios were slightly greater in September (rising water season) in the Aripuanã and Acari Rivers, which indicated some hydrological influence.

The $^{87}Sr/^{86}Sr$ ratios of the studied rivers are among the highest recorded in Amazonia (Gaillardet et al., 1997; Santos et al., 2014) and worldwide (Gaillardet et al., 1999) (Fig. 6) and exceed 0.735, which is the average for the Amazon craton (Allègre et al., 1996). The low $^{87}Sr/^{86}Sr$ ratios of the Aripuanã River resemble those of the Trombetas River, which flows through the eastern portion of the granitic-gneissic and volcanic Brazilian craton (Hieronymus et al., 1993).

4.4. $\delta^{18}O$ and δD values

The river waters have higher isotopic values in September and November (S/11 and N/12) and lower isotopic values in March and April (M/13, A/13, Fig. 7A and Supplementary Data Files). Fig. 7B compares the isotopic compositions of the studied rivers and meteoric waters from Amazonia (stations of Benjamin Constant, São Gabriel, Manicoré, Manaus, Santarém, Marabá and Porto Velho) that were retrieved from the GNIP dataset (IAEA, 2014) to identify evaporative processes in the rivers. The Amazon meteoric water line (AMWL) has a slope of 7.8 and an intercept of 11.3, which is very similar to the local (Apuí) meteoric water line (ApMWL, Honório et al., 2010), with a slope of 8.28 and an intercept of 10.69. Higher $\delta^{18}O$ and δD values in the local rainwater were observed during the dry season (July and September) (Honório et al., 2010).

The isotopic values observed in the river waters covered a much narrower range than those in the meteoric water, and most of these values were plotted to the right of the AMWL and ApMWL. The slopes of the rivers range between 3.02 and 5.81, which are lower than those of the MWLs. Thus, evaporation influenced some of the samples collected during September and November (Fig. 7B and Supplementary Data Files), when higher temperatures occurred in the Amazon region. This slight evaporative effect is more intense in the Jatuarana, Ig1, Acari and Sucunduri Rivers, which indicates no relationships with the size/discharge of the rivers. However, a strong link is observed with the climatic cycle. For instance, the highest $\delta^{18}O$ and δD values occur in September and November, which mark the end of the dry season, whereas the lowest values occur in March and April, which mark the end of the high water season. Additionally, the small Ig1 River has $\delta^{18}O$ and δD values that are similar to those in the large Sucunduri River. Fig. 7A shows that the curve of isotopic values is out of phase with the meteoric water curves by two to three months. Throughout the year, the constant isotopic composition of the groundwater ($\delta^{18}O = -5‰$ and $\delta D = -36‰$, Table 3) indicates the groundwater has a minimal influence on the $\delta^{18}O$ and δD values of the river water compared with the meteoric water.

In Fig. 7 B, the samples with higher δD values and higher d excess values (from 19 to 23) are plotted above AMWL and LMWL.

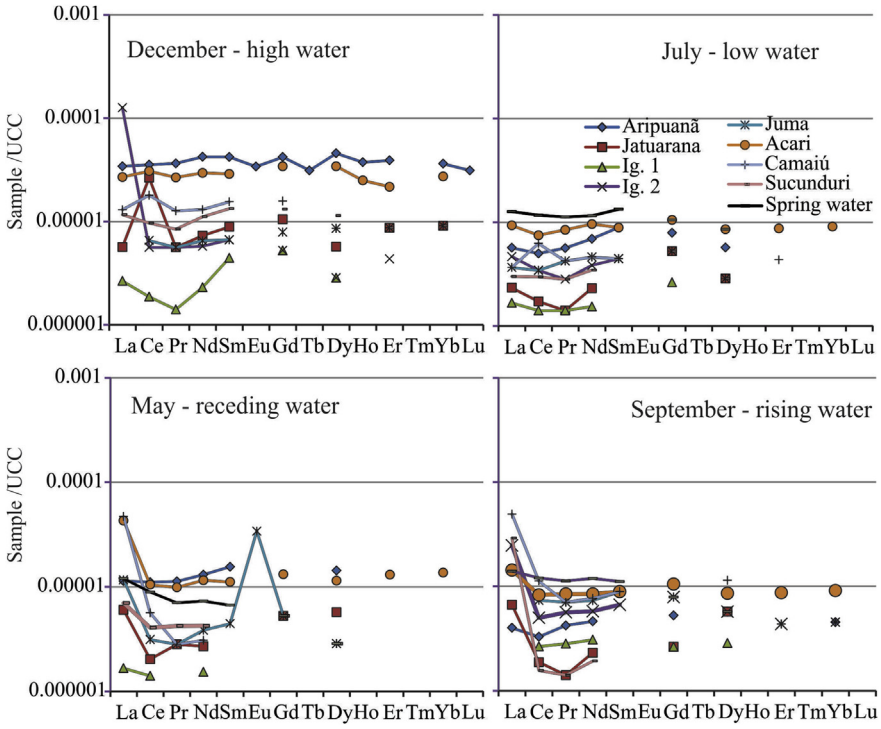

Fig. 5. Rare earth elements normalized to the estimated average composition of the upper crust (UCC, Taylor and McLennan, 1985).

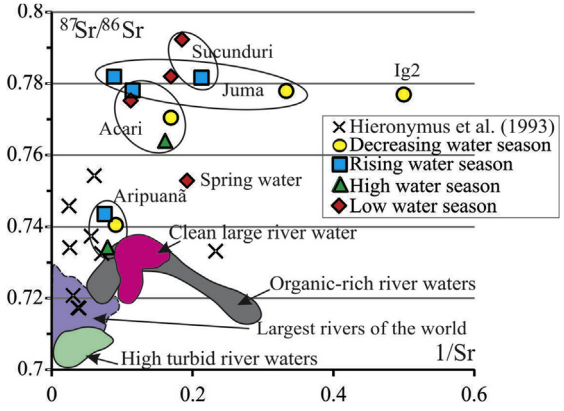

Fig. 6. $^{87}Sr/^{86}Sr$ ratios as a function of 1/Sr (Sr in μg L^{-1}) and compared with the ratios observed in other rivers from Amazonia and around the world (Hieronymus et al., 1993; Gaillardet et al., 1997, 1999 and Santos et al., 2014).

These samples define a river water line for the period of higher discharge that has a slope of 7.54 and an intercept of 17.4 (Fig. 7B). The increase in the δD values is likely related to water vapor recycling, which plays a major role in the Amazon water cycle (Gat and Matsui, 1991; Victoria et al., 1991; Martinelli et al., 1996). Available estimates indicate that 25%–40% of Amazon rainfall returns to the atmosphere by evapotranspiration (Gat and Matsui, 1991; Leopoldo et al., 1982). This water vapor has high d excess values.

5. Discussion

5.1. Environmental influences

To determine the geology influence were calculate the atmospheric contribution. From the total major dissolved elements weighted by rainwater, on average, 14% of the Na^+ in the Acari River and 100% of the Na^+ in the Jatuarana River originate from the atmosphere (Table 1). This atmospheric influence is strongest during the high water season (from October to April), when 100% of the Na^+ in the Camaiú River originates from the atmosphere. In addition, atmospheric Na^+ inputs account for 21–38% of the SO_4^{2-} concentration and 2–19% of the Mg^{2+} concentration in the rivers. The atmospheric contributions of the other dissolved ions (H^+, K^+, Ca^{2+}, TAlk and NO_3^-) and SiO_2 were negligible.

The average of each major dissolved element and TDS weighted by the monthly rainwater amount after correcting for atmospheric contributions and using cluster analysis, shows there are two groups of river waters (Fig. 8A): i) the Aripuanã and Acari Rivers, which drain a large area with a variable bedrock composition (including siliciclastic sedimentary rocks, felsic volcano-sedimentary rocks and intrusive felsic rocks with minor basic rocks) and have the most concentrated waters, and ii) the other rivers, which mostly drain areas with siliciclastic sedimentary bedrock. In the second cluster, two secondary clusters are identified, one including Ig1 and Ig2, which are the smallest rivers with the most dilute water and highest variability, and one including the Jatuarana, Juma, Camaiu and Sucunduri Rivers.

The cluster analysis of the trace element compositions using the same conditions as those of the major dissolved element and TDS, determined that Al, Fe, Mn and Zn identifies nearly the same clusters of river water (Fig. 8B), although the Jatuarana River is more similar to the Aripuanã and Acari Rivers. Less abundant trace elements, such as Sr, Rb, Y, and Ba, also identify the same two groups. The Acari and Aripuanã Rivers have higher Sr, Rb and Ba concentrations (the Sucunduri River also has high Ba) than most of the other sampled rivers (Fig. 9). Compared with large organic-rich rivers from Amazonia and central Africa, which also flow over cratonic terrain and through forested regions, and other turbid rivers from Amazonia (Hieronymous et al., 1993; Allègre et al., 1996; Gaillardet et al., 1997, 1999; Viers et al., 2000; Sondag et al., 2010; Sanchez et al., 2015), the trace elements as well as the

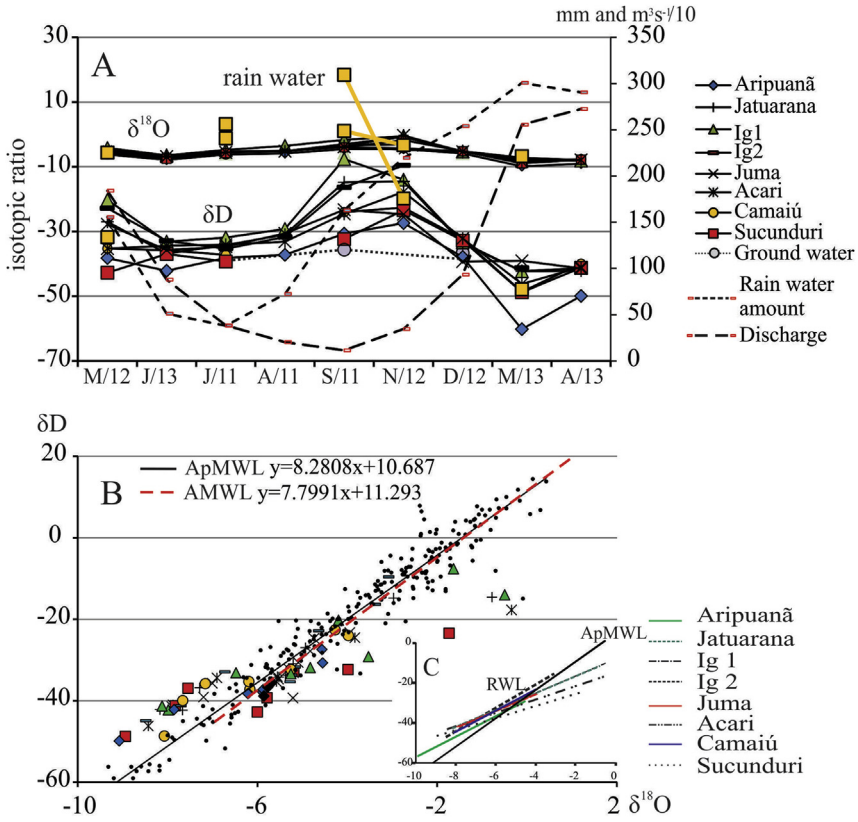

Fig. 7. A- Monthly $\delta^{18}O$ and δD variation; B- $\delta^{18}O$ versus δD values of the studied river waters compared with the meteoric water of the Benjamin Constant, São Gabriel, Manicoré, Manaus, Santarém, Marabá and Porto Velho Rivers, which are all in Amazonia (IAEA, 2014). ApMWL-regression line of the local meteoric water (Honório et al., 2010), AMWL-regression line of the Amazon meteoric water; C- regression lines for each type of river water (RWL).

major dissolved elements and TDS indicates the studied rivers flow through areas with geochemistry that is unique to the local Brazilian craton. The weathering of this local silicate Proterozoic and Paleozoic felsic volcano-sedimentary rocks and intrusive felsic rocks with minor basic rocks and siliciclastic sedimentary rocks of the Brazilian craton, exerts large spatial variability in the studied river waters composition and in the high K^+ content, as well as in the abundance of Sr, Rb, Y, Ba, Mn, Cu and Zn and the radiogenic Sr isotopic ratios. Thus, the dominance of K^+ result from the local bedrock, which is rich in K-bearing minerals, such as feldspar and mica that have higher K_2O contents than Na_2O contents (CPRM, 2013), but the inland positions of these rivers may also exerts some chemical control. The Aripuanã River Basin, which probably have few ^{87}Rb-rich silicate minerals, may explain the low $^{87}Sr/^{86}Sr$ ratios (0.734115–0.743457) in this river relative to the other studied rivers (0.763901–0.79225). However, some process of dilution may also control the Sr isotopes as indicate Santos et al. (2014) for the Amazon basin.

The local bedrock influence is also highlighted when compared with the 60 largest rivers around the world (Gaillardet et al., 1999) as is exemplified by the Na-normalized molar data (Mg/Na from 0.25 to 8.26 and Ca/Na from 0.48 to 6.1, Table 1 and Fig. 10). The local felsic volcano-sedimentary rocks and intrusive felsic rocks with minor basic rocks contain minerals were more prone to weathering and cause the higher TDS in the Aripuanã and Acari River relative to the siliciclastic sedimentary environments of the other rivers. The higher Na-normalized molar data in the Ig1 and Sucunduri Rivers (Fig. 10), although may indicate some carbonate influence, also highlight the role of atmospheric Na^+ contributions in these rivers (Table 2), which increases the Mg/Na and Ca/Na ratios after atmospheric correction.

The dominance of TAlk relative the sum of cations (Fig. 11) is another important characteristic of rivers that drain forests areas like the studied rivers, relative to most highly turbid rivers in Amazonia, where a close correlation is observed between the sum of cations and TAlk (e.g., Mortatti and Probst, 2003 and Moquet et al., 2011) or the cation concentrations are high (Sondag et al., 2010). Higher TAlk in the spring water, especially in August and September (Supplementary data files), indicates that the soil is rich in dissolved organic compounds derived from the oxidation of vegetation and that these compounds enter the hydrosphere via groundwater. In addition, the higher acidity and NO_3^- concentrations in the spring water likely result from the influences of the soil and the siliciclastic sedimentary rocks.

The climate of the studied region, which dictates greater discharge during the high water season, exerts temporal control over the river water chemistry and over the amount of recycled water vapor, besides the significant atmospheric Na^+, SO_4^{2-}, and Mg^{2+} contributions (up to 100% of the Na^+ in the Jatuarana and Camaiú River). The recycled water vapor result in isotopic values plotted above the MWL (Fig. 7A) at the end of the high-water season. The size of the basin is also important for controlling the chemical composition because the small Ig1 and Ig2 rivers have lower chemical loads than the Jatuarana, Juma, Camaiu and Sucunduri Rivers, as all of them drain the same sedimentary rock.

5.2. . Weathering rates

The local weathering profiles, which isolate the bedrock and produce kaolinite and gibbsite (Silva et al., 2012), correspond with

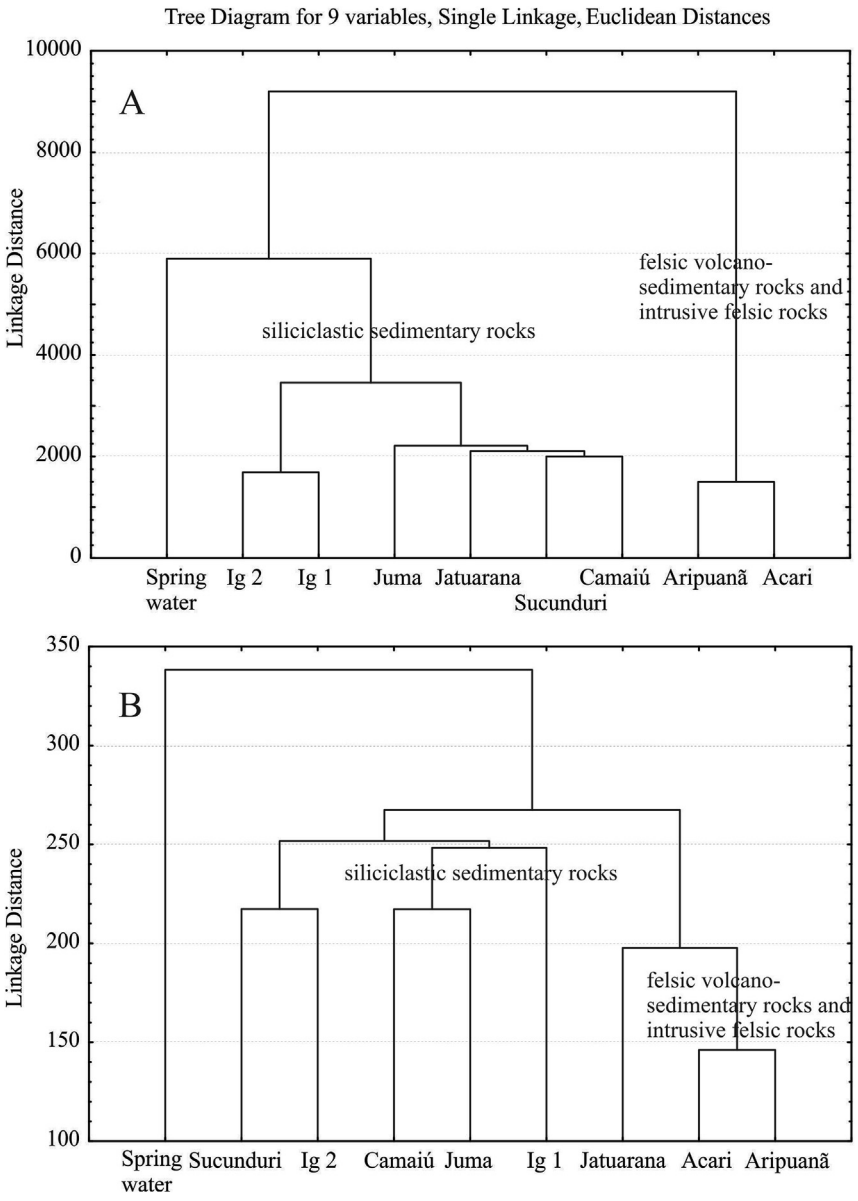

Fig. 8. Cluster analysis performed using single linkage and Euclidian distance techniques. A-using the average of each major dissolved element and TDS weighted by the monthly rainwater amount, and B- using Al, Fe, Mn and Zn, which are the most concentrated trace elements, weighted by the monthly rainwater amount.

calculated weathering indexes of between 1.7 and 3.8 ($(3Na^{+}+3K^{+}+1.25Mg^{2+}+2Ca^{2+}\text{-}SiO_2)/(0.5Na^{+}+0.5K^{+}+0.75Mg^{2+}+Ca^{2+})$ of Boeglin and Probst (1998)). These indexes correspond with the highly leached oxisols and spodosols that cover large areas of the cratonic terrain in Amazonia (Bravard and Righi, 1989; Dubroeucq and Volkoff, 1998 and Horbe et al., 2004). This environment and the high amounts of organic acid derived from the forested catchments produce water with a high concentration of dissolved SiO_2 and TAlk. However, the concentration of dissolved SiO_2 (which averages 6.1 mg L^{-1}, Table 1) is lower than the average concentration in rivers worldwide (10.8 mg L^{-1}, Meybeck et al., 1996), indicating that the studied river waters are very dilute. This dilution results in low annual CWRs of between 1.75 and 4.15 t km^{-2} yr^{-1} and in a low weathering front in the local bedrock of between 0.62 and 1.5 m Ma^{-1}. The slightly higher CWRs observed during the high water season and the higher weathering rate in the Aripuanã River (of 8.74 t km^{-2} yr^{-1} and 3.16 m Ma^{-1}, respectively) reinforce the influences of local siliciclastic rock weathering on the chemical compositions of river waters.

The calculated CWR values are among the lowest in the world, as shown in Fig. 12A, and correspond with the CWR values of rivers from colder regions with lower runoff, such as the Canadian and Siberian cratons, as reported by Millot et al. (2002) and Zakharova et al. (2007). This fact supports the minimal influence of temperature on river water chemistry in the study area.

The CO_2 consumption rates, which were calculated using the sum of cations after atmospheric contributions, vary between 21.54 and 60.51 10^3 mol km^{-2} yr^{-1}. Similar to the CWF values, the CO_2 consumption rates are higher in the Aripuanã River (Table 3). This indicates that the CO_2 consumption rates are sensitive to the drainage of felsic to basic igneous and metamorphic bedrock relative to siliciclastic sedimentary bedrock (Tables 1 and 3), which corresponds with previous results at a global scale (Dessert et al., 2003). The high discharge/runoff during the high water season is also correlated with a much higher CO_2 consumption rate relative

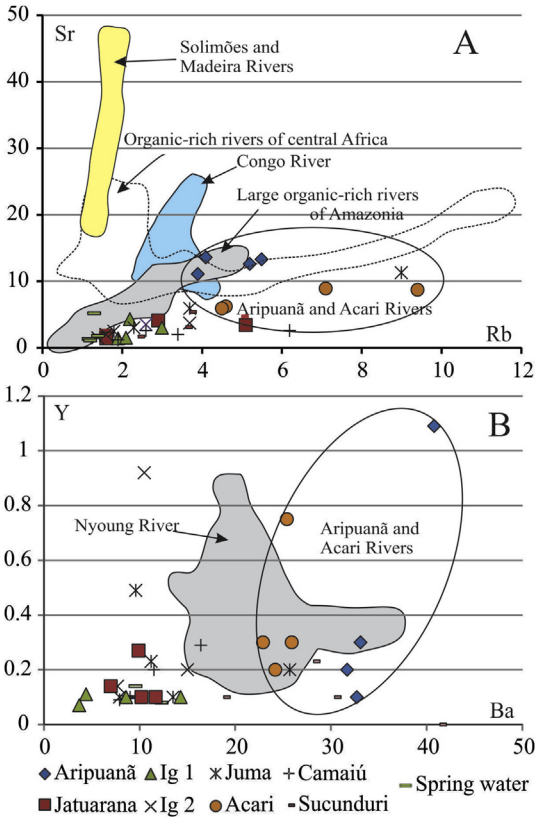

Fig. 9. A- Sr as a function of Rb (both in μg L^{-1}) for the samples compared with the more turbid Solimões and Madeira rivers, other organic-rich rivers from Amazonia (Gaillardet et al., 1997), and other large organic-rich rivers from central Africa (Allègre et al., 1996, Viers et al., 2000). B– Y as a function of Ba (both in μg L^{-1}) compared with the organic-rich Nyoung river water from Africa (Viers et al., 2000).

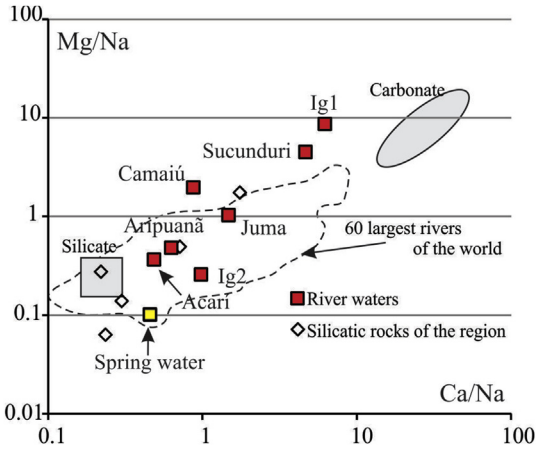

Fig. 10. A- Plot of the Na-normalized molar ratios (in μmol L^{-1}) after correcting for atmospheric contributions and compared with the silicate and carbonate end-member reservoirs from Gaillardet et al. (1997), which contain siliciclastic rocks, and 60 large rivers around the world (Gaillardet et al., 1999). For this plot the monthly Na, Ca and Mg concentrations of the samples were weighted by the amount of monthly rainfall.

to the low water season (Table 3), which agrees with the results of Mortatti and Probst (2003) and with results from other rivers around the world (Hartmann et al., 2014). The CO_2 consumption rates observed in this study are lower than those in the larger and more turbid Solimões and Amazonas Rivers but higher than those in other organic rivers in Amazonia (Fig. 12B). The rates are also

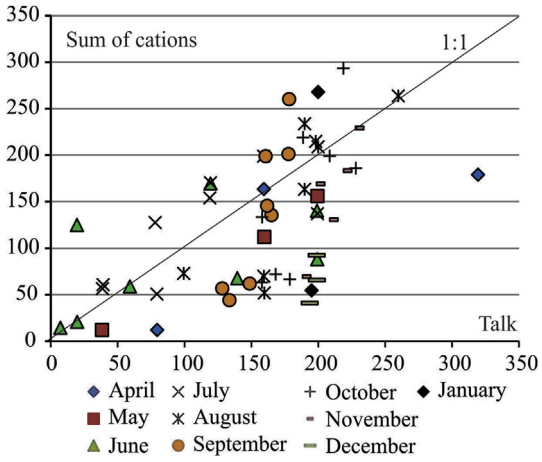

Fig. 11. Plot of the sum of cations and total alkalinity (TAlk) (both in μg L^{-1}) after correcting for atmospheric contributions.

similar to those of the Madeira River, which contains more turbid water (Gaillardet et al., 1997). The CO_2 consumption rates in the study area also resemble the rates in the Niger, Congo and Zaire Rivers, which flow through a similar lateritic cratonic terrain in Africa (Gaillardet et al., 1999) (Fig. 12).

Here, we present a first-order estimate of the CWF value and CO_2 consumption rate for the entire craton by extrapolating our results to the craton surface of the Amazon Basin (the total craton area is 2.5106 km2, and the total Amazon Basin area is 6106 km^2). We compare these results with the flux of the Amazon River at Óbidos station. The craton terrain would contribute approximately 13% of the CWR transported by the Amazon River if we only consider cations + SiO_2 as described by Gaillardet et al. (1997). However, the craton terrain would contribute up to 15% of the CWR if we consider cations + SiO_2+TAlk as described by Mortatti and Probst (2003). The CO_2 consumption from weathering of the craton region would represent between 9% and 11% of the total CO_2 consumption (associated with carbonate and silicate weathering) in the Amazon Basin at Óbidos station (Gaillardet et al., 1997, Mortatti and Probst, 2003) and could reach 17%–24% if we only consider the CO_2 consumption flux that is associated only with silicate weathering. Although the CWR rate strengthens the steady state erosion model for the Amazon craton, the CO_2 consumption rate indicates that weathering of the cratonic terrain, which produces leached oxisols and spodosols, remains an important consumer of CO_2.

6. Conclusions

Based on new time series of river water chemistry, we provide an accurate estimate of the chemical composition of small and medium organic-rich river waters flowing over cratonic substratum covered by lateritic soils in Amazonia. The environmental conditions in Amazonia, which can be extrapolated to other tropical areas, generate acidic and dilute waters dominated by TAlk, SiO_2 and K^+. Several factors control the chemical compositions of the rivers: 1) the hydrologic regime controls the H^+ and TAlk; 2) the meteoric water contributions, including some evaporative effects, control the $\delta^{18}O$ and δD values and most of the Na^+ concentration; 3) the abundances of K^{2+}, Sr, Rb, Y, Ba, Mn, Cu and Zn and the radiogenic Sr isotopic ratios illustrate the contributions of bedrock, which varies from felsic to basic igneous and metamorphic to siliciclastic sedimentary rocks; 4) the size of the basin control the low chemical loads in the small rivers; and 5) the minimal influence of

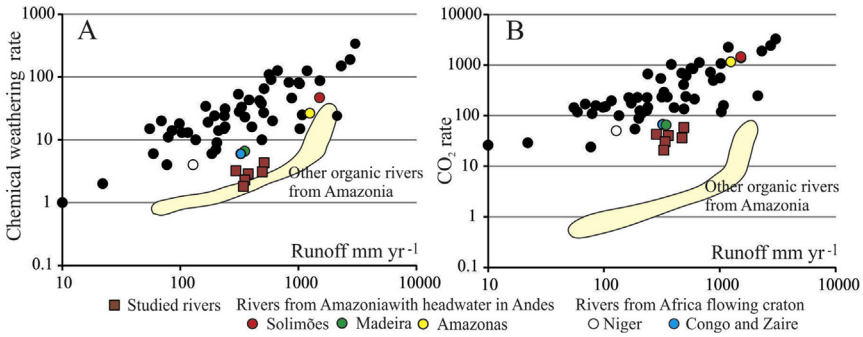

Fig. 12. A- Chemical weathering rate (CWR in t km^{-2} yr^{-1}) and B– CO_2 consumption rate (10^3 mol km^{-2} yr^{-1}) relative to runoff (mm yr^{-1}). Black points represent the 60 largest rivers around the world (Gaillardet et al., 1999) and the other colored points represent other organic rivers from Amazonia (Gaillardet et al., 1997).
For interpretation of the references to colour in this figure legend, the reader is referred to the web version of this article.

groundwater on the river water chemistry relative to rain water, explains the highly dilute composition relative to most of the rivers of the world. The low export of dissolved ions and the low weathering rate support a steady state erosion model for the Amazon craton. However, the CO_2 consumption by weathering is higher than expected and indicates bedrock control.

Acknowledgments

This research was supported by CNPq (Conselho Nacional de Desenvolvimento Científico e Tecnológico, grant no. 620039/2008-6, 302296/2010-0 and 471971/2010-3. A. S. Lages thanks CAPES (Coordenação de Aperfeiçoamento de Pessoal de Nível Superior) for awarding him a scholarship. We also thank the anonymous referees that provided helpful suggestions for improving the manuscript.

Appendix A. Supplementary data

Supplementary data related to this article can be found at http://dx.doi.org/10.1016/j.apgeochem.2015.10.007.

References

Allégre, C.J., Dupré, B., Négrel, P., Gaillardet, J., 1996. Sr-Nd-Pb isotopes systematics in Amazon and Congo River systems: constrain about erosion processes. Chem. Geol. 131, 93–112.
Bardossy, G., Aleva, G.J.J., 1990. Lateritic bauxites. In: Developments in Economic Geology, vol. 27. Elsevier, Amsterdam.
Barroux, G., Sonke, J.E., Boaventura, G., Viers, J., Godderis, Y., Bonnet, M.-P., Sondag, F., Gardoll, S., Lagane, C., Seyler, O., 2006. Seasonal dissolved rare earth elements dynamics of the Amazon River main stem, its tributaries, and the Curuaí floodplain. Geochemistry. Geophys. Geosystems 7. http://dx.doi.org/10.1029/2006GC001244.
Berner, E.K., Berner, R.A., 1987. The Global Water Cycle: Geochemistry and Environment. Englewood Clifs, New Jersey, 397 pp.
Boeglin, J.-L., Probst, J.-L., 1998. Physical and chemical weathering rates and CO_2 consumption in a tropical lateritic environment: the upper Niger Basin. Chem. Geol. 148, 137–156.
Bravard, S., Righi, D., 1989. Geochemical differences in an Oxisol-Spodosol toposequence of Amazônia. Braz. Geoderma 44, 29–42.
Callède, J., Guyot, J.L., Ronchail, J., L'Hôte, Y., Niel, H., Oliveira, E., 2004. Évolution du débit de l'Amazone à Óbidos de 1903 à 1999. Hydrological Sci. J. 49, 85–97.
CPRM Companhia de Pesquisas e Recursos Minerais, 2013. Geologia e recursos minerais da folha Sumaúma – SB.20-Z-D. Projeto Sumaúma-Roosevelt-Mutum. Relatório Final. MME/SGTM. CPRM, Manaus, 260 pp.
Dessert, C., Dupré, B., Gaillardet, J., François, L.M., Allégre, C.J., 2003. Basalt weathering laws and the impact of basalt weathering on the global carbon cycle. Chem. Geol. 202, 257–273.
Dubroeucq, D., Volkoff, B., 1998. From Oxisols to Spodosols and Histosols, evolution of the soil mantles in the Rio Negro Basin (Amazonas). Catena 32, 245–280.
Dupré, B., Gaillardet, J., Rousseau, D., Allegre, C.J., 1996. Major and trace elements of River-Borne material: the Congo Basin. Geochimica Cosmochimica Acta 60, 1301–1321.
Edmond, J.M., Palmer, M.R., Measures, C.I., Stallard, R.F., 1996. The fluvial geochemistry and denudation rate of the Guayana Shield in Venezuela, Colombia and Brazil. Geochimica Cosmochimica Acta 59, 3301–3325.
Gaillardet, J., Dupré, B., Allègre, C.J., Négrel, P., 1997. Chemical and physical denudation in the Amazon River Basin. Chem. Geol. 142, 141–173.
Gaillardet, J., Dupré, B., Louvat, P., Allègre, C.J., 1999. Global silicate weathering and CO_2 consumption rates deduced from the chemistry of large rivers. Chem. Geol. 159, 3–30.
Gaillardet, J., Viers, J., Dupré, B., 2007. Trace element in river waters. In: Drever, J.I. (Ed.), Surface and Ground Water, Weathering, and Soils. Treatise on Geochemistry. Pergamon, pp. 225–272.
Gat, J.R., Matsui, E., 1991. Atmospheric water balance in the Amazon basin: an isotopic evapotranspiration model. J. Geophys. Res. Atmos 96 (D7), 13179–13188 (1984–2012).
Gupta, P., Noone, D., Galewsky, J., Sweeney, C., Vaughn, B.H., 2009. Demonstration of high-precision continuous measurements of water vapor isotopologues in laboratory and remote filed deployments using wavelength-scanned cavity ring-down spectroscopy (WS-CRDS) technology. Rapid Commun. Mass Spectrom. 23, 2534–2542.
Hartmann, J., Moosdorf, N., Lauerwald, R., Hinderer, M., West, J., 2014. Global chemical weathering and associated P-release – the role of lithology, temperature ans soil properties. Chem. Geol. 363, 145–163.
Hieronymus, B., Godot, J.M., Boulegué, J., Bariac, T., Negrel, P., Dupré, B., 1993. Chimie du fleuve Tocantins et de revieres cotieres de l'este du Para (Brésil). Grands Bassins Fluviaux, Paris, pp. 357–374.
Honório, B., Horbe, A.M.C., Sayler, P., 2010. Chemical composition of rainwater in Western Amazonia - Brazil. Atmos. Res. 98, 416–425.
Horbe, A.M.C., Horbe, M.A., Kenitiro, S., 2004. Tropical spodosols in northeastern amazonas state, Brazil. Geoderma 119, 55–68.
IAEA, 2014. International Atomic Energy Agency. Access October 2014. www.iaea.org.
Leopoldo, P.R., Franken, W., Matsui, E., Salati, E., 1982. Estimativa da evapotranspiração de floresta Amazônica de Terra-Firme. Acta Amaz. 12, 23–28.
Martinelli, L.A., Victoria, R.L., Sternberg, L.S.L., Ribeiro, A., Moreira, M.Z., 1996. Using stable isotopes to determine sources of evaporated water to the atmosphere in the Amazon basin. J. Hydrol. 183, 191–204.
Meybeck, M., 1983. Atmospheric inputs and river transport of dissolved substance. In: Webb, B.W. (Ed.), Dissolved Loads of Rivers and Surface Water Quantity/Quality Relationships. IAHS, Hamburg, pp. 173–192.
Meybeck, M., Friedrich, G., Thomas, R., Chapman, D., 1996. Rivers, Water Quality Assessments, a Guide to the Use of Biota, Sediments and Water in Environmental Monitoring. Chapman and Hall, London.
Milliman, J.D., Syvitski, J.P.M., 1992. Geomorphic/Tectonic Control of Sediment Discharge to the Ocean: the Importance of Small Mountainous Rivers, 100. The Journal of Geology, pp. 525–544.
Millot, R., Gaillardet, J., Dupré, B., Allegre, C.J., 2002. The Global control of silicate weathering rates and the coupling with physical erosion: new insights from rivers of the Canadian Shield. Earth Planet. Sci. Lett. 196, 83–98.
Moquet, J.-S., Crave, A., Viers, J., Seyler, P., Armijos, E., Bourrel, L., Chavarri, E., Lagane, C., Laraque, A., Casimiro, W.S.L., Pombosa, R., Noriega, L., Vera, A., Guyot, J.-L., 2011. Chemical weathering and atmospheric/soil CO_2 uptake in the Andean and foreland Amazon basins. Chem. Geol. 287, 1–26.
Moquet, J.S., Viers, J., Crave, A., Armijos, E., Lagane, C., Lavado, W., Pepin, E., Pombosa, R., Noriega, L., Santini, W., Guyot, J.L., 2014. Comparison between silicate weathering and physical erosion rates in Andean basins of Amazon River. In: Procedia Earth & Planetary Science. Presented at the Geochemistry of the Earth's Surface GES 10, pp. 275–279. Paris France.
Mortatti, J., Probst, J.L., 2003. Silicate rock weathering and atmospheric/soil CO_2 uptake in the Amazon Basin estimated from river water geochemistry, seasonal and spatial variations. Chem. Geol. 197, 177–196.
Oliva, P., Viers, J., Dupré, B., 2003. Chemical weathering in granitic environments. Chem. Geol. 202, 225–256.
Reis, N.J., 2006. Projeto rochas carbonáticas de Apuí - Amazonas. Relatório Final. CPRM. Serviço Geológico do Brasil, Manaus, 60 pp.

Sanchez, L., Horbe, A., Moquet, J.S., Sondag, F., Guyot, J.L., 2015. Variação espaço-temporal do material inorgânico dissolvido na bacia Amazônica. Acta Amaz. 45, 175–186.

Santos, R.V., Sondag, F., Cochonneau, G., Lagane, C., Brunet, P., Hattingh, K., Chaves, J.G.S., 2014. Source Area and Seasonal $^{87}Sr/^{86}Sr$ Variations in Rivers of the Amazon Basin. Hydrological Processes (Published online in Wiley Online Library).

Silva, P.M., Horbe, A.M.C., Horbe, M.A., 2012. Mineralogia e geoquímica de ocorrências manganesíferas da bacia Alto Tapajós, sudeste do estado do Amazonas, Brasil. Boletim do Museu Paraense Emílio Goeldi. Ciências Nat. 7, 11–28.

Sioli, H., 1968. Hydrochemistry and geology in the Brasilian amazon region. Amazoniana 3, 267–277.

Sondag, F., Guyot, J.L., Moquet, J.S., Laraque, A., Adele, G., Cochonneau, G., Doudou, J.C., Lagane, C., Vauchel, P., 2010. Suspended sediment and dissolved load budgets of two Amazonian rivers from Guiana Shield, Maroni river at Langa Tabiki and Oyapock river at Saut Maripa (French Guiana). Hydrol. Process. 24, 1433–1445.

Stallard, R.F., Edmond, J.M., 1983. Geochemistry of the Amazon 2. The influence of geology and weathering environment on the dissolved load. J. Geophys. Res. 88, 9671–9688.

Stallard, R.F., Edmond, J.M., 1987. Geochemistry of the Amazon 3. Weathering chemistry and limits to dissolved contributions. J. Geophys. Res. 92, 8293–8302.

Tardy, Y., Roquin, C., 1998. Dérive des continents Paléoclimats et alterations tropicales. Èditions BRGM, Orléans, France.

Taylor, S.R., McLenann, S.M., 1985. The Continental Crust its Composition and Evolution. Blackwell Scientific Publications, Oxford, 312pp.

Viers, J., Dupré, B., Braun, J.-J., Deberdt, S., Angeletti, B., Ngoupayou, J.N., Michard, A., 2000. Major and trace elements abundance, and strontium isotopes in the Nyong basin rivers (Cameroon), constraints on chemical weathering processes and elements transport mechanisms in humid tropical environments. Chem. Geol. 169, 211–241.

Victoria, R.L., Martinelli, L.A., Mortatti, J., Richey, J., 1991. Mechanisms of water recycling in the Amazon Basin: isotopic insights. Ambio 20, 384–387.

Xu, Z., Lui, C.-Q., 2010. Water geochemistry of the Xijiang basin Rivers, South China, chemical weathering and CO_2 consumption. Appl. Geochem. 25, 1603–1614.

Zakharova, E.A., Pokrovsky, O.S., Dupré, B., Gaillardet, J., Efimova, L.E., 2007. Chemical weathering of silicate rocks in Karelia region and Kola Peninsula, NW Russia: assessing the effect of rock composition, wetlands and vegetation. Chem. Geol. 242, 255–277.